SOLAR MICROWAVE BURSTS FROM ELECTRON POPULATIONS WITH A 'BROKEN' ENERGY SPECTRUM

J. HILDEBRANDT[1], A. KRÜGER[1], I. M. CHERTOK[2], V. V. FOMICHEV[2] and R. V. GORGUTSA[2]

[1]*Astrophysikalisches Institut Potsdam, An der Sternwarte 16, D-14482 Potsdam, Germany*

[2]*IZMIRAN, Troitsk, Moscow Region, 142092, Russia*

(Received 9 June 1997; accepted 27 February 1998)

Abstract. Usually the gyrosynchrotron emission of microwave bursts from electron populations with a power-law (PL) energy distribution has been considered under the assumption that the spectral index of the distribution is constant over a wide range of energies. Meanwhile, there is strong evidence, in particular from hard X-ray and γ-ray, but also from cm/mm wavelength radio observations, that in many solar flare events the spectrum of the emitting electrons is characterized by a significant hardening at energies above 100–500 keV. We present some examples of calculated microwave burst spectra at cm/mm wavelengths taking into account the above evidence. It is shown that a break in the energy spectrum of the PL electrons can indeed result in a spectral hardening sometimes observed in microwave bursts at frequencies above 10–30 GHz.

1. Introduction

In a previous paper (Chertok *et al.*, 1995; hereafter Paper I) radio burst spectra have been analysed in the range 3–80 GHz, using measurements of the observatories at Bern and Nobeyama supplemented by data from worldwide network stations. It was found that there exists an extended group of events exhibiting a spectral flattening at millimeter wavelengths. In particular, three types of flattening are mainly observed: (1) a high-frequency flattening following a monotonic spectral flux increase at cm-wavelengths; (2) a broad-band spectrum forming a flat apex at mm-wavelengths; (3) a millimetric flattening by a decrease of the slope (i.e., a hardening) of the descending branch of the spectrum having a peak in the microwave range. Besides this, in complex bursts a strong temporal evolution of millimeter spectra may occur resulting in either type of flattening. Some varieties of the high frequency flattenings were found also in a number of preceding studies (cf., e.g., Hachenberg and Wallis, 1961; Croom, 1973; Shimabukuro, 1970; Kaufmann *et al.*, 1985; and other references given in Paper I) as well as in a recent review by Kaufmann (1996). A few possibilities capable of producing millimeter flattening were considered in Paper I: (i) multiple source regions of gyrosynchrotron radiation, (ii) a two-component ('broken') energy spectrum of the emitting high-energy electrons, (iii) a temporal hardening of the electron spectrum during extended flares,

Solar Physics **181:** 337–349, 1998.

and (iv) optically thin bremsstrahlung of hot evaporated plasma. The latter process was discussed there in more detail.

In the present paper, we pay attention mainly to the role of a 'broken' energy spectrum of the emitting electrons (item (ii) mentioned above), producing radio spectra with a peak in the microwave range and a weaker decrease above a characteristic break frequency ν_b in the mm-range (type (3) hardening; cf., Figures 1(c), 1(d), 2, and 4 of Paper I). It should be noted that radio bursts with such a type of spectral hardening are rather common (cf., e.g., Kucera *et al.*, 1993; Akimov *et al.*, 1996; Gorgutsa, 1996; Kaufmann, 1996; and Paper I).

The main evidence for high-energy particle spectra with non-constant power-law (PL) indexes comes from hard X-ray and γ-ray observations (cf., e.g., Bai and Ramaty, 1976). The SMM measurements with HXRBS and GRS demonstrated that there are flare events in which the observed emission spectrum in the 20 keV $-$20 MeV photon energy range cannot be described by a single PL function (cf., Dennis, 1988; Vestrand, 1988; McTiernan and Petrosian, 1991; Li, 1995). According to these measurements, a double PL spectrum seems to be a better fit to the data with a break at energies $E_b \approx 300$ keV, the negative spectral index at $E < E_b$ being significantly larger ($\lambda_1 \approx 4.3$) than that at $E > E_b$ ($\lambda_2 \approx 2.2$).

Similar results were found by Li and Hurley (1995) in their statistical studies of the BATSE/CGRO data. Their findings are as follows: (a) the distribution of E_b displays considerable dispersion, ranging from 50 to 750 keV, with a mean value at about 200 keV; (b) the negative spectral index above E_b is less than that below the break energy, with a difference of $\lambda_1 - \lambda_2 \approx 2.8$; (c) only a very weak trend of center-to-limb decrease can be found for these parameters. Further evidence for 'broken' hard X-ray/γ-ray spectra came from the GRANAT/PHEBUS measurements (Barat *et al.*, 1994).

It should be mentioned that there exist also a considerable number of hard X-ray spectra showing 'downward' breaks at comparatively low energies ($E < 100-150$ keV) reported, e.g., by Lin and Schwartz (1987), Dulk, Kiplinger, and Winglee (1992), and others. However, this kind of spectral softening observed together with a weak temporal hardening (i.e., an increase of E_b) in the course of a burst will certainly not affect the resulting radio spectrum, least of all in the mm-wavelength range which we are particularly interested in. Therefore, we will restrict our present consideration to the hardening of the instantaneous (peak) hard X-ray/γ-ray spectra.

A spectral hardening of the X-ray/γ-ray spectra seems to be indicative of a corresponding hardening of the energy spectrum of the non-thermal electrons. The cause of this hardening is unclear, but there are reasons to believe that it is due to the flare acceleration process (McTiernan and Petrosian, 1991). It is evident that this form of electron spectra must influence also the optically thin part of the gyrosynchrotron radiation at mm-wavelengths. The purpose of the present study is to analyse this possible influence by means of model calculations of radio burst spectra. In Section 2, a general description of our model is presented, whereas

Section 3 is devoted to the results obtained and their discussion. Conclusions are given in Section 4.

2. Model

The calculations are based on a complex but very general and geometrically simple model, allowing us to simulate different source conditions and to include the contributions of all relevant direct emission mechanisms (gyroresonance absorption and Coulomb bremsstrahlung of the thermal background plasma as well as gyrosynchrotron radiation of the nonthermal (PL) electrons). To calculate the escaping radiation from a given emission volume, we insert the expressions of the relevant absorption and emission coefficients in our code to compute the transfer of radiation along the ray path, taking into account also influences of the ambient medium (propagation effects, Razin suppression, etc.). For slightly inhomogeneous sources approximated by a multi-layer model, we use the solution of the equation of radiative transfer for one layer as initial value for the next one:

$$I_{\nu,\sigma}(k) = \frac{n_\sigma^2(k)}{n_\sigma^2(k-1)}\, I_{\nu,\sigma}(k-1)\, \mathrm{e}^{-\mu_\sigma(k)L_k} + \frac{j_{\nu,\sigma}(k)}{\mu_{\nu,\sigma}(k)}\,[\,1 - \mathrm{e}^{-\mu_\sigma(k)L_k}], \tag{1}$$

where $I_{\nu,\sigma}$ is the intensity, n_σ is the refractive index, $j_{\nu,\sigma}$ and $\mu_{\nu,\sigma}$ are emission and absorption coefficients, respectively, $\sigma = \pm 1$ is the magnetoionic mode, $L = \sum_{k=1}^{m} L_k$ is the total thickness of all m layers, and $I_{\nu,\sigma}(0) = 0$.

The relevant $j_{\nu,\sigma}$ and $\mu_{\nu,\sigma}$ of gyrosynchrotron radiation are vector integrals of the product of the rather complicated volume emissivity of a gyrating particle and the distribution function (or its derivative, respectively) over the velocity. In the isotropic case, after a transformation into an only energy-dependent integral, the energy distribution function $u(\varepsilon)$ mainly determines the resulting expressions ($\varepsilon = E/(m_0c^2)$ is the normalized energy). Assuming a PL distribution function, it can be written by

$$u(\varepsilon) = A_N\, \varepsilon^{-\lambda} \qquad \text{for} \qquad \varepsilon_1 < \varepsilon < \varepsilon_2 \tag{2}$$

with

$$A_N = \frac{(\lambda - 1)\,(\varepsilon_1\, \varepsilon_2)^{\lambda-1}}{\varepsilon_2^{\lambda-1} - \varepsilon_1^{\lambda-1}} \tag{3}$$

as normalization constant resulting from the condition

$$\int_{\varepsilon_1}^{\varepsilon_2} \mathrm{d}\varepsilon\, A_N \varepsilon^{-\lambda} = 1. \tag{4}$$

This type of PL distribution will be denoted here as 'single' PL. In order to model the above-mentioned 'broken' or 'double' PL, we superimpose two 'single' PL functions with different λ:

$$u(\varepsilon) = u_1(\varepsilon) + u_2(\varepsilon) \tag{5}$$

with

$$u_1(\varepsilon) = A_{N1}\,\varepsilon^{-\lambda_1} \qquad \text{for} \qquad \varepsilon_1 < \varepsilon < \varepsilon_b, \tag{6}$$

$$u_2(\varepsilon) = A_{N2}\,\varepsilon^{-\lambda_2} \qquad \text{for} \qquad \varepsilon_b \leq \varepsilon < \varepsilon_2, \tag{7}$$

where $\lambda_1 > \lambda_2$ ('flattening' of the spectrum).

A_{N1} and A_{N2} are calculated such that $u(\varepsilon)$ is normalized according to Equation (4) and continuous, i.e.,

$$A_{N1}\,\varepsilon_b^{-\lambda_1} = A_{N2}\,\varepsilon_b^{-\lambda_2}. \tag{8}$$

All PL functions of this kind have a low-energy cut-off, i.e., they are, strictly speaking, physically unrealistic and used as an approximation in the measured energy range. We tried to solve this problem by fitting the low-energy boundary ε_1 (which is often not well determined) to the thermal background plasma. Assuming that the number densities of the thermal and nonthermal particles are given, the low-energy boundary can be estimated using the normalization and continuity conditions.

Taking into account this fact and assuming a 'single' PL, we find that the resulting spectra will depend on the following 8 parameters:

B – magnetic field strength,
N_0 – number density of the thermal (background) plasma,
θ – angle between the magnetic field vector and the line of sight,
L – thickness of the emission volume (in the line-of-sight direction),
T – temperature of the (background) plasma,
N – number density of the nonthermal electrons,
ε_2 – high-energy boundary of the PL distribution,
λ – PL index.

In the case of a 'broken' PL, λ turns into λ_1 (low-energy PL index), and two further parameters must be introduced, viz.,

ε_b – energy where the PL distribution is broken,
λ_2 – PL index of the high-energy particles,

so that finally 10 parameters may influence the spectrum.

As input for the homogeneous model (1 layer) we have to choose one parameter set, whereas for the inhomogeneous case m parameter sets have to be modeled. After carrying out the radiative transfer, we obtain for each given frequency the escaping intensity. In order to compare such a spectrum with observed spectra we have to convert it into flux density units by assuming an effective area of emission A_{eff} by the relation

$$F_\nu = \frac{A_{\text{eff}}}{R_{\text{SE}}^2}\,I_\nu \;\longrightarrow\; F_\nu[\text{s.f.u.}] \approx 0.45\,A_{\text{eff}}\,I_\nu \tag{9}$$

(R_{SE}, Sun–Earth distance).

It should be mentioned that the PL spectral indexes of the emitting electrons ($\lambda_{1,2}$) may differ from the observed indexes of the hard X-ray/γ-ray emission ($\delta_{1,2}$). As is known, e.g., for a thick-target source, the index of the electron distribution is $\lambda = \delta + 1$ (cf., e.g., Brown, 1971; Syrovatsky and Shmeleva, 1972).

3. Results of Model Calculations and Discussion

3.1. Reference spectra

Let us start with the homogeneous case ($m = 1$) which will be useful for a better recognition of how variations of each parameter influence the resulting spectrum. Our 'standard' parameters, around which the variations will be scattered, are similar to those derived in Paper I:

$N_0 = 5 \times 10^{15}$ m^{-3},	$N = 10^{12}$ m^{-3},
$L = 15$ Mm,	$\lambda_1 = 4.5$,
$B = 700$ G,	$\lambda_2 = 2.1$,
$\theta = 45°$,	$\varepsilon_b = 1.4$ ($E_b \approx 200$ keV),
$T = 8 \times 10^6$ K,	$\varepsilon_2 = 6$ ($E_2 \approx 3$ MeV).

Figure 1 shows flux density spectra separately calculated for gyrosynchrotron radiation (light solid), gyroresonance absorption (dotted), and Coulomb bremsstrahlung (dashed), as well as the resultant radio spectra for two different PL distributions of nonthermal electrons (heavy solid lines). It should be noted that the strong gyroabsorption effects (harmonic structure) at the optically thick part of the radio spectrum are a consequence of the assumed homogeneous model for the magnetic field in the radio source (cf., e.g., Zheleznyakov and Zlotnik, 1980; Willson, 1983) and will be suppressed (smoothed) in the inhomogeneous case (see Subsection 3.5. and Figure 4). Therefore, we will focus our preliminary consideration mainly on that part of the spectrum ($\nu \gtrsim \nu_{peak}$) where the typical behaviour is well reflected even for homogeneous sources.

One can see from Figure 1 that for the parameters chosen the optically thin gyrosynchrotron radiation dominates at cm/mm wavelengths. As could be expected (cf. Dulk, 1985), the slope of this part of the frequency spectra strongly depends on the PL index λ. For a 'single' PL distribution, the decrease of λ (hardening) results in a corresponding hardening of the radio spectra (cf., Figures 1(a) and 1(b)). As a consequence, a 'broken' energy spectrum (i.e., a combination of two different PL spectra) should cause a 'broken' radio spectrum. For example, from Figure 1(c) one can see that a change of the electron spectral index from $\lambda_1 = 4.5$ to $\lambda_2 = 2.1$ at $E_b \sim 200$ keV yields a 'broken' radio spectrum with $\alpha_1 \approx 3.8$, $\alpha_2 \approx 1.3$, and a break frequency $\nu_b \approx 16$–17 GHz. Such a radio spectrum is similar to observed spectra (see Paper I). For further discussion of the influence of

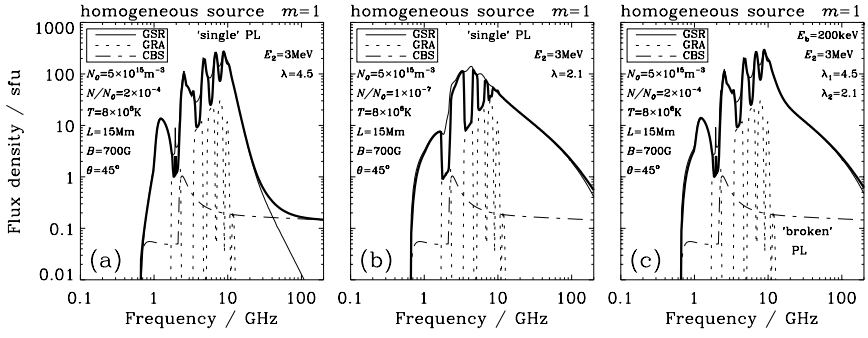

Figure 1. Calculated radio spectra for homogeneous source conditions: (a) and (b) for 'single' PL distributions, but with soft ($\lambda = 4.5$) and hard ($\lambda = 2.1$) energy spectra (and, correspondingly, different particle number densities); (c) for a composite ('broken') PL electron spectrum. The light curves show the spectra which would be generated if each possible emission mechanism is considered separately (GSR, gyrosynchrotron radiation; GRA, gyroresonance absorption; CBS, Coulomb bremsstrahlung), the heavy curves show the resultant radio spectra. The parameters assumed are indicated in the figures.

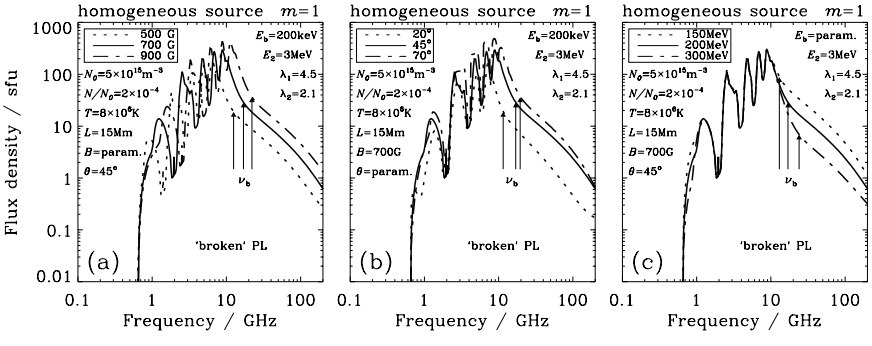

Figure 2. Calculated radio spectra for the homogeneous case ($m = 1$), demonstrating the influence of selected source parameters: (a) magnetic field strength; (b) viewing angle; (c) break energy. The solid curve in each figure belongs to the reference spectrum (thick line in Figure 1(c)). The relevant values for the varying parameter corresponding to each curve are given in the box at the left upper corner. The break frequency is marked by an arrow.

various source parameters, the resultant radio spectrum shown in Figure 1(c) will be used as a reference spectrum.

3.2. VARIATIONS OF THE BREAK FREQUENCY

It is useful to start with a consideration of some general features of gyrosynchrotron emission from PL electrons (Dulk and Marsh, 1982; Dulk, 1985). Supposing that there are two populations of superthermal electrons with number densities N_1, N_2, and PL indexes λ_1, λ_2 ($\lambda_1 > \lambda_2$) in the source, a comparison of the relevant

gyrosynchrotron emissivities on the basis of the approximation given by Dulk and Marsh (1982) yields the following expression for the break frequency ν_b:

$$\frac{\nu_b}{\nu_g} = 10^{-0.577}\ (\sin\theta)^{0.722}\ \left(\frac{N_1}{N_2}\right)^{1.11/(\lambda_1-\lambda_2)}, \tag{10}$$

where ν_g is the electron gyrofrequency.

Equation (10) shows that ν_b depends on B, θ, and the parameters of the PL electron populations N_1, N_2, λ_1, and λ_2. It should be noted that in our model the correlation between N_1, N_2, λ_1, and λ_2 in Equation (10) is connected with E_b via the normalization and continuity conditions (cf., Equation (8)) in such a manner that for given λ_1 and λ_2 the increase (decrease) of the ratio N_1/N_2 corresponds to an increase (decrease) of E_b. Thus, it is clear that the break frequency depends mainly on B, θ, and E_b. The results of our extended calculations confirm this conclusion (see Figure 2; here and hereafter the reference spectrum is shown by a solid line).

The increase of ν_b from $\sim$ 12–13 GHz (for $B = 500$ G) to $\sim$ 22–23 GHz (for $B = 900$ G) in Figure 2(a) reflects the general displacement of the gyrosynchrotron spectrum towards higher frequencies (shifting of the gyroharmonics) and an increase of the intensity with increasing magnetic field strength.

The dependence of ν_b on θ is due to its strong influence on the opacity of gyrosynchrotron emission. For decreasing angles, the optical depth becomes smaller (the argument of the Bessel functions in the emissivity formula is proportional to $\sin\theta$). Consequently, this results in a decrease of the break frequency (from $\nu_b \sim 21$–22 GHz for $\theta = 70°$ to $\nu_b \sim 11$–12 GHz for $\theta = 20°$ in Figure 2(b)), as well as in a general decrease of the gyrosynchrotron flux density (less influence of higher harmonics).

Furthermore, it is reasonable that an increase of E_b is accompanied by an increase of ν_b, corresponding to the following values in our case (Figure 2(c)): $\sim$14–15 GHz (for $E_b = 150$ keV) and $\sim$ 24–25 GHz (for 300 keV). An additional effect – the decrease of the gyrosynchrotron emission at $\nu < \nu_b$ – results from the normalization condition. For larger E_b, the number of electrons with $E > E_b$ becomes essentially smaller and so their contribution to the gyrosynchrotron emission too.

3.3. VARIATIONS OF THE SPECTRAL INDEXES

Changes of B, θ, and E_b, outlined in the previous section, exert influence on the break frequency, but do not alter significantly the spectral indexes of the 'broken' radio spectra. However, these indexes and the occurrence of the radio break strongly depend on the parameters of the energy spectrum of the emitting electrons.

It is clear that an increase (decrease) of λ_1 and λ_2 leads to a corresponding increase (decrease) of the radio indexes α_1 and α_2 (Figures 3(a) and 3(b)). The break in the radio spectrum takes place only if the difference between the low- and high-energy indexes is sufficiently large, for example, if $\lambda_1 - \lambda_2 \gtrsim 2$. Then, the number of the high-energy electrons with $E > E_b$ and their contribution to the

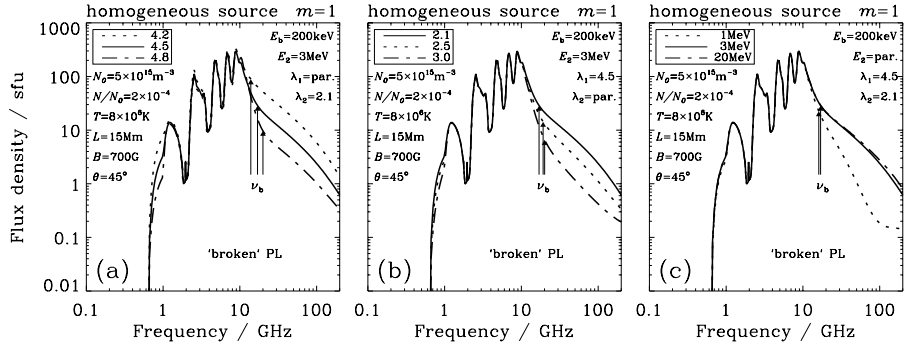

Figure 3. Examples of calculated resultant radio spectra for the homogeneous model ($m = 1$) demonstrating the influence of selected source parameters: (a) low-energy PL index; (b) high-energy PL index; (c) upper energy boundary. Other notations are the same as in the previous figure.

gyrosynchrotron emission should be sufficiently large. On the other hand, it is not surprising that the radio break becomes less visible when the upper boundary of the PL electron distribution E_2 decreases and approaches the same order of magnitude as E_b (dotted curve in Figure 3(c)).

3.4. OTHER INFLUENCES

There are a number of source parameters whose influence on the 'broken' radio spectra is either sufficiently clear or not too strong. This allows us to explain the corresponding regularities without figures.

The increase of the density of the thermal background plasma N_0 leads to, first of all, a strong increase of the flux density of the optically thin bremsstrahlung at high frequencies. However, for the parameters used here and not too high frequencies ($\nu < 100$ GHz), the gyrosynchrotron radiation remains predominate. Secondly, due to the assumed constancy of the ratio N/N_0, the absolute density of the nonthermal electrons N rises also. As a consequence, the gyrosynchrotron emissivity enhances remarkably, but the resultant form of the 'broken' radio spectrum remains practically unchanged. The same occurs when the thickness of the emission volume increases (in addition, the assumption that $A_{\rm eff} = 2.5 \times L^2$ reinforces this tendency for the flux density spectrum).

Variations of the density of the nonthermal particles act mainly on the gyrosynchrotron intensity as a whole but not on the characteristic shape of the radio spectrum. The same takes place when the temperature of the background plasma rises, since, due to the normalization condition, this leads to a displacement of the low-energy boundary E_1 of the PL distribution towards higher energies, and, consequently, to a corresponding increase of the mean energy of the PL electrons. For illustration, assuming $T \approx 8 \times 10^6$ K and $N/N_0 \approx 2 \times 10^{-4}$ as used in most of our calculations, the normalization and continuation conditions yield a low-energy boundary $E_1 \approx 10$ keV.

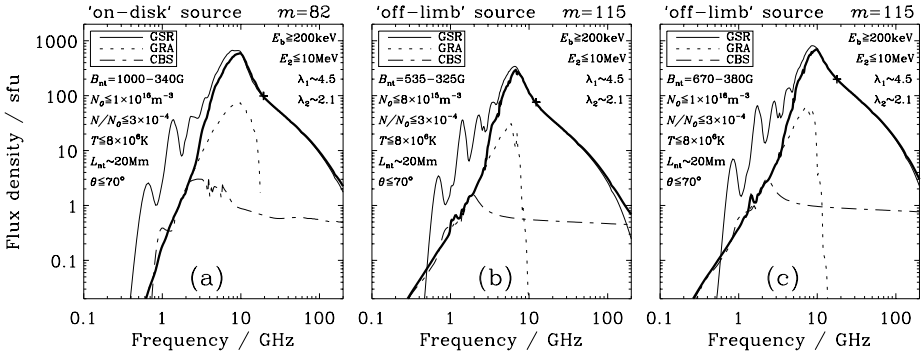

Figure 4. Examples of calculated intensity spectra using inhomogeneous parameter distributions along the line of sight: (a) 'on-disk' source, (b) and (c) 'off-limb' sources with slightly different parameter configurations. The break frequency is marked by a '+'. Further explanations are given in the text.

3.5. INHOMOGENEOUS SOURCES

For more detailed simulations, the model allows us to calculate also the radiation from inhomogeneous sources using a multi-layer approximation along the ray path. Depending on the parameter distributions along the line of sight ($\boldsymbol{B}(z)$, $N_0(z)$, $T(z)$, ...), two different configurations can be distinguished: 'on-disk' sources (the observer looks through the source towards the solar disk) and 'off-limb' sources (the observer looks through the source which is outside the limb). In the first case, contributions from chromospheric levels (thermal bremsstrahlung) are also possible, which would result in an increase of the intensity spectrum at mm waves, where the corona becomes optically thin.

Observed spectra are mostly given in s.f.u. which requires the knowledge of $A_{\rm eff}$ in order to convert the calculated intensity values into flux density values. This parameter is, in particular for inhomogeneous sources, probably not constant over the whole frequency range and will be different for gyrosynchrotron emission and bremsstrahlung too, especially in the 'on-disk' case. Because of these uncertainties, it would be better to use intensities for presenting our calculated spectra, but for comparison with observations (and with the spectra shown before), we tried to avoid these problems by substracting the 'background radiation' that will be emitted outside the flare source from the total radiation. The conversion into flux units was done afterwards, using an effective area $A_{\rm eff} = 2.5 L_{\rm eff}^2$, similar to the homogeneous case considered before, but now with $L_{\rm eff}$ being the 'nonthermal' part of L (see below). The flux values so obtained must be taken as an upper limit because this implies the assumption of horizontal homogeneity over $A_{\rm eff}$, which is certainly not fulfilled.

Generally, one should expect that variations of the main parameters in the inhomogeneous source will erode or mask the break in the resultant radio spectra. However, as Figure 4 illustrates, this is not the case, at least for the parameter

sets taken in our examples. Although nearly all parameters changed slightly from layer to layer, the break appears now as ever in all three spectra computed for an 'on-disk' source (Figure 4(a)) as well as for two 'off-limb' sources with slightly different parameters (Figures 4(b) and 4(c)). Source (b) may be located at a higher altitude than source (c) because of its weaker magnetic field ($B \approx 535$–340 G and $B \approx 670$–380 G, respectively). The parameter ranges, e.g., for B, given in the legend of Figure 4, cover only the nonthermal part $L_{\rm eff}$ of the whole ray path; the total length L taken into account exceeds 10^5 km! As for the homogeneous sources, the increase of the magnetic field strength results in a rise of the break frequency from $\nu_b \sim 11$ GHz (b) to $\nu_b \sim 15$ GHz (c).

The reason for such a maintenance of the radio break also in inhomogeneous spectra is that the main contribution to the radio emission, especially in the optically thin part of the spectrum, comes from the central region of the source where the density and the energy of the nonthermal particles have their maximum values. More detailed investigations will be published elsewhere (Hildebrandt *et al.*, 1998).

A remarkable difference compared with the homogeneous case is the more smoothed behaviour at the optically thick part of the spectrum coming from the slightly changing B (overlapping of harmonics) which leads therefore to a suppression of the GSR not only by reabsorption of the nonthermal electrons themselves but also to a stronger thermal gyroresonance absorption of the background plasma because of its lower brightness temperature (cf. light solid curves – light dotted curves – heavy solid curves in Figure 4). The still-existing harmonic structure for the GSR even in the inhomogeneous case (light solid lines), is caused by the limited range of B inside $L_{\rm eff}$. The question whether such 'cyclotron lines' can be observed and used for diagnostics of the magnetic field in the source region was discussed by Willson (1983). It seems to us that a (theoretically possible) detection of this phenomenon is very unlikely, in particular for only thermal conditions. Since, in general, the magnetic field strength decreases monotonically with height, such a necessary abrupt change of optical thickness can only be caused by strongly inhomogeneous plasma conditions occurring, for instance, in small, dense, and very hot (or nonthermal) sources. Apart from these circumstances, one needs an instrument with very high spatial and spectral resolution.

3.6. SOME ADDITIONAL ESTIMATIONS

The results of our model calculations with respect to a possible 'break' in the radio spectra reveal that for reasonable parameter variations the ratio of the break frequency to the electron gyrofrequency is kept in the restricted range of $\nu_b/\nu_g \approx 7$–9. Furthermore, it can be stated that the break only appears when the difference between the spectral indexes of the emitting electrons is large enough ($\lambda_1 - \lambda_2 \gtrsim 2$). Taking into account these basic results and assuming $\theta \sim 45^{\rm o}$ as a typical angle, we can make some additional estimations.

From Equation (10) follows that the ratio of the number densities of the low-energy (soft) and high-energy (hard) sub-populations of the emitting electrons is $N_1/N_2 \approx (0.6–1) \times 10^3$.

A 'broken' microwave spectrum can be observed, if the ν_b is less than the critical frequency ν_*, introduced in Paper I (Equation (5)), where the contribution of bremsstrahlung begins to exceed that of gyrosynchrotron radiation. This condition leads to the following inequality:

$$\frac{N_1}{N_2} < 10^{12.7} \left(\frac{B\,N}{N_0^2} \right)^{0.76} . \tag{11}$$

Then, for $N_1/N_2 \approx 10^3$ (see above), $N/N_0 \approx 2 \times 10^{-4}$, and $B \approx 700$ G it follows that the number density of the thermal (background) plasma N_0 must be less than 10^{11} cm^{-3}. This means, that the stage of flare events, when the dense evaporated plasma fills in the flare loops and mm-bremsstrahlung achieves its maximum, turns out to be the least favorable one to find a break in the radio spectrum.

4. Conclusions

The results of our model computations presented here show that particles with a 'broken' PL energy spectrum, revealed by hard X-ray/γ-ray measurements during bursts, may, in principle, cause a radio spectrum which exhibits a clearly marked 'break' in the optically thin part of the gyrosynchrotron emission.

Assuming typical values for the high-energy electrons ($\lambda_1 \approx 4–5.5$, $\lambda_2 \approx 2.1–3.5$, $\lambda_1 - \lambda_2 \gtrsim 2$, $E_b \approx 100–500$ keV), and reasonable plasma parameters inside the radio source (e.g., $B \approx 300–1000$ G), the calculated frequency of the microwave break corresponds to the observations, i.e., ranges at 10–30 GHz.

It should be noted that, in principle, the observed 'broken' spectrum both in the hard X-ray and microwave ranges can be formed as a result of superposition of radiation from two sources, each of which has its own 'single' PL spectrum and, perhaps, other differing parameters. However, the possible existence of an electron population with a 'broken' energy spectrum, resulting from the flare acceleration process, should also be considered. It is quite clear that a combination of spectral radio observations and measurements with sufficiently high spatial resolution in wide hard X-ray/γ-ray and radio ranges is necessary to study this problem in further detail. A first example of such an approach has been given by Bai and Ramaty (1976); recently, Silva *et al.* (1997) studied a special flare using multifrequency observations and found also a double PL as the best fit for the spectra. According to the hard X-ray observations, there is not only the energy break of the instantaneous (for example, peak) spectra, but also a clear temporal hardening of the spectra during extended events (cf., e.g., Kiplinger, 1995).

It is evident, that a 'broken' energy spectrum of the emitting electrons can scarcely explain other spectral trends towards higher frequencies than a spectral

hardening of the gyrosynchrotron radiation considered in the present paper. This statement belongs, for example, to burst spectra with fluxes increasing for shorter micro/mm wavelengths discussed by Kaufmann (1996) in terms of the model of a primeval explosive compact synchrotron source. A further explanation of such a spectral flattening at higher frequencies may be due to thermal optically thin bremsstrahlung of dense hot (perhaps, evaporated) plasma (Ohki and Hudson, 1975; Paper I). Free-free absorption of gyrosynchrotron radiation as a possible origin of flat spectra proposed by Ramaty and Petrosian (1972) is, in principle, included in our code. But the results of our model calculations did not confirm this effect of flattening for plausible inhomogeneous parameter conditions.

The whole picture of the radio spectra may be still more complicated, in particular because real microwave bursts seem to consist of numerous elementary spikes with time scales down to milliseconds, as revealed by observations with high temporal resolution. These elementary spikes are often not 'in phase' at different cm/mm wavelengths (see, e.g., Kaufmann, 1996, for a review). The radio spectra considered here are, of course, averaged over these fast time structures.

It should be remarked that, besides the possible break at 10−30 GHz discussed above, a further spectral flattening at still higher frequencies will take place due to the transition from optically thin gyrosynchrotron radiation to optically thin bremsstrahlung. The observation of such extended radio burst spectra may become possible in the near future, for example, when the new submillimeter-wave telescope (SST) will come in operation at El Leoncito Astronomical Complex in Argentina (Kaufmann *et al.*, 1994).

Acknowledgements

The authors are grateful to an anonymous referee for useful criticism and suggestions. The Russian authors acknowledge the support from the Russian Foundation of Basic Research and the Russian Federal Astronomical Program. They would like to thank also Prof. K. H. Rädler for the invitations to stay at the Astrophysical Institute Potsdam and for hospitality. Furthermore, we are indebted to Dr A.V. Stepanov for his critical reading of the manuscript and for fruitful discussions. This work was also supported by the Deutsche Agentur für Raumfahrtangelegenheiten (DARA) under Grant No. 50 QL 9602.

References

Akimov, V. V., Ambrož, P., Belov, A. V., Berlicki, A., Chertok, I. M., Karlický, M., Kurt, V. G., Leikov, N. G., Litvinenko, Yu. E., Magun, A., Minko-Wasiluk, A., Rompolt, B., and Somov, B. V.: 1996, *Solar Phys.* **166**, 107.

Bai, T. and Ramaty, R.: 1976, *Solar Phys.* **49**, 343.

Barat, C., Trottet, G., Vilmer, N., Dezalay, J.-P., Talon, R., Sunyaev, R., Terekhov, O., and Kuznetsov, A.: 1994, *Astrophys. J.* **425**, L109.
Brown, J. C.: 1971, *Solar Phys.* **18**, 489.
Chertok, I. M., Fomichev, V. V., Gorgutsa, R. V., Hildebrandt, J., Krüger, A., Magun, A., and Zaitsev, V. V.: 1995, *Solar Phys.* **160**, 181 (Paper I).
Croom, D. L.: in R. Ramaty and R. G. Stone (eds.), 'Solar Millimeter-Wave Bursts', *High Energy Phenomenon on the Sun*, NASA/GSFC Symposium, September 28–30, 1972, Publ. NASA SP-342, p. 114.
Dennis, B. R.: 1988, *Solar Phys.* **118**, 49.
Dulk, G. A.: 1985, *Ann. Rev. Astron. Astrophys.* **23**, 169.
Dulk, G. A. and Marsh, K. A.: 1982, *Astrophys. J.* **259**, 350.
Dulk, G. A., Kiplinger, A. L., and Winglee, R. M.: 1992, *Astrophys. J.* **389**, 756.
Gorgutsa, R. V.: 1996, *Izv. RAN, Ser. Fizicheskaya* **60**, 154.
Hachenberg, O. and Wallis, G.: 1961, *Z. Astrophys.*, **52**, 42.
Hildebrandt, J., Krüger, A., Stepanov, A. V., and Zaitsev, V. V.: 1998, in preparation.
Kaufmann, P.: 1996, *Solar Phys.* **169**, 377.
Kaufmann, P., Correia, E., Costa, J. E. R., Zodi Vas, A. M.: 1985, *Nature* **313**, 380.
Kaufmann, P., Parada, N.J., Magun, A., Rovira, M., Ghielmetti, H., and Levata, H.: 1994, *Proc. Kofu Symposium 'New look at the Sun'*, 1993, Kofu, Japan, NRO Report **360**, 323.
Kiplinger, A. L.: 1995, *Astrophys. J.* **453**, 973.
Kucera, T. A., Dulk, G. A., Kiplinger, A. L., Winglee, R. M., Bastian, T. S., and Graeter, M.: 1993, *Astrophys. J.* **412**, 853.
Li, P.: 1995, *Astrophys. J.* **443**, 855.
Li, P. and Hurley, K.: 1995, in *Proc. 24th Int. Cosmic Ray Conf., Rome* **4**, 110.
Lin, R. P. and Schwartz, R. A.: 1987, *Astrophys. J.* **312**, 462.
McTiernan, J. M. and Petrosian, V.: 1991, *Astrophys. J.* **379**, 381.
Ohki, K. and Hudson H. S.: 1975, *Solar Phys.* **43**, 405.
Ramaty, R. and Petrosian, V.: 1972, *Astrophys. J.* **178**, 241.
Shimabukuro, F. I.: 1970, *Solar Phys.* **15**, 424.
Silva, A. V. R., Gary, D. E., White, S. M., Lin, R. P., and De Pater, I.: 1997, *Solar Phys.* **175**, 157.
Stepanov, A. V., Urpo, S., and Zaitsev, V. V.: 1992, *Solar Phys.* **140**, 139.
Syrovatsky, S. I. and Shmeleva, O. P.: 1972, *Astron. Zh.* **49**, 334.
Vestrand, W. T.: 1988, *Solar Phys.* **118**, 95.
Willson, R. F.: 1983, *Solar Phys.* **89**, 103.
Zheleznyakov, V. V. and Zlotnik, E. Ya.: 1980, *Solar Phys.* **68**, 317.